

# Design of novel, potent, and selective human $\beta$ -tryptase inhibitors based on $\alpha$ -keto-[1,2,4]-oxadiazoles

Chang-Sun Lee,\* Weili Liu, Paul A. Sprengeler, John R. Somoza, James W. Janc, David Sperandio, Jeffrey R. Spencer, Michael J. Green and Mary E. McGrath

*Departments of Chemistry and Biology, Celera, 180 Kimball Way, South San Francisco, CA 94080, USA*

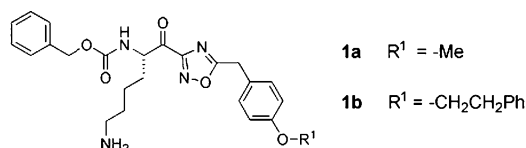
Received 23 March 2006; revised 2 May 2006; accepted 2 May 2006

Available online 22 May 2006

**Abstract**—A series of novel  $\alpha$ -keto-[1,2,4]-oxadiazoles has been synthesized as human tryptase inhibitors for evaluation as a new class of anti-asthmatic agent. The inhibitor design is focused on using a prime-side hydrophobic pocket and the S2 pocket of  $\beta$ -tryptase to achieve inhibition potency and selectivity over other serine proteases.  
© 2006 Elsevier Ltd. All rights reserved.

Interest in tryptase as a therapeutic target for asthma has increased following the proof of principle studies with APC-366 in sheep and humans.<sup>1</sup> Tryptase is a homotetrameric serine protease with trypsin-like specificity that is stored in mast cell granules and released upon IgE stimulation.<sup>2</sup> The proteolytic activity of tryptase is believed to be responsible for immediate- and long-term effects that contribute to the physiological effects experienced by asthma sufferers.<sup>3</sup> Therefore, inhibiting tryptase with potent, selective, and preferably oral small molecule drugs could have important therapeutic value.<sup>4</sup> Several groups have identified small molecule inhibitors of tryptase as potential drugs for asthma.<sup>5</sup> However, designing compounds that selectively inhibit tryptase over antitargets such as trypsin has proven difficult.

Although we achieved good tryptase inhibition potency with **1b** containing a phenyl ether linkage, compounds in the series had at least three problems: poor trypsin selectivity, low kinetic solubility, and high hERG K<sup>+</sup> channel binding affinity (Fig. 1).<sup>6</sup> We therefore turned our attention to other linkages to improve not only anti-target selectivity but also physicochemical properties such as solubility and log *P*.<sup>7</sup> We first designed compounds **6**



Compounds	$\beta$ -Tryptase K <sub>i</sub> (nM)	Trypsin K <sub>i</sub> (nM)	selectivity	solubility( $\mu$ M) at pH 7.4	hERG inhib. % at 1 $\mu$ M
<b>1a</b>	770	22	0.03	348	ND
<b>1b</b>	12	35	3.0	23	40

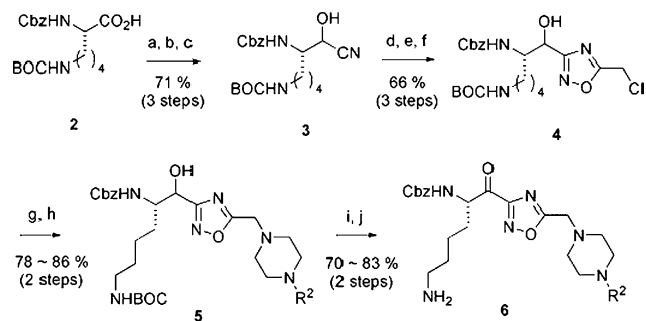
**Figure 1.** Tryptase inhibitors containing an activated ketone as a warhead.

containing a piperazine linker, which should have higher solubility relative to **1b**.

The synthesis of the inhibitors **6** is outlined in Scheme 1. Protected (L)-Lys **2** was converted to **3** by reduction of Weinreb amide and hydrocyanation reaction with acetone cyanohydrin. Compound **3** was transformed to the corresponding hydroxyamidine,<sup>8</sup> which was coupled with 2-chloroacetylchloride. Thermal intramolecular cyclization of the coupling product provided the [1,2,4]-oxadiazole ring **4**.<sup>9</sup> Compound **4** was converted to **5** by N-alkylation with an excess amount of piperazine followed by the second N-alkylation/N-acylation with alkyl/acyl halides. The alcohols **5** were oxidized under Swern conditions,<sup>10</sup> and final deprotection of the BOC group from the lysine side chain provided the series of compounds **6**.

**Keywords:** Tryptase inhibitor; Asthma; Activated carbonyl; Oxadiazole.

\* Corresponding author. Tel.: +1 925 242 0501; e-mail: [csleesammy@gmail.com](mailto:csleesammy@gmail.com)



**Scheme 1.** Reagents and conditions: (a) MeNHOMe, HATU, DMF; (b)  $\text{LiAlH}_4$ , THF, 0 °C; (c) acetone cyanohydrin,  $\text{CH}_2\text{Cl}_2$ ; (d)  $\text{NH}_2\text{OH}$ , EtOH; (e)  $\text{ClCH}_2\text{COCl}$ ,  $\text{CHCl}_3$ ; (f) 100 °C, DMF; (g) piperazine,  $\text{K}_2\text{CO}_3$ ,  $\text{CH}_3\text{CN}$ ; (h)  $\text{R}^2\text{-Cl}$ ,  $\text{K}_2\text{CO}_3$ ,  $\text{CH}_3\text{CN}$ ; (i)  $(\text{COCl})_2$ , DMSO, TEA,  $\text{CH}_2\text{Cl}_2$ ; (j) HCl; (g)  $\text{CH}_3\text{CN}$ .

Table 1 shows the tryptase inhibition potency for compounds **6a–e**. Both **6a** and **6b** have similar activities as **1a**, suggesting that the linker groups may not be long enough to reach to the prime-side binding pocket. Increasing the chain length by one methylene, as in **6c**, increases potency by 7-fold. Replacing the carbonyl group of **6b** by a methylene **6d** or an ethylene **6e** increases potency further by 21- and 40-fold, respectively, indicating that the piperazine modification has successfully allowed the phenyl group to reach the distal pocket of the prime side.

As expected, kinetic solubility of most compounds was high. Compared with **1b**, the piperazine linkage increases solubility of **6c–e** by at least 15-fold. The X-ray co-crystal structure of tryptase with **6c** (Fig. 2) clearly shows the phenyl end cap group occupying the prime-side hydrophobic binding pocket.<sup>13</sup> To our delight, **6c** also had significantly reduced hERG  $\text{K}^+$  channel binding affinity (2.3% at 10  $\mu\text{M}$  concentration) relative to ether-containing compound **1b**, suggesting that the amide might be a focal point for further optimization. In order to improve poor trypsin selectivity and microsomal stability of **6c**, we then adopted the benzamide linkage as shown in the series of compounds **10** for the inhibitor design.

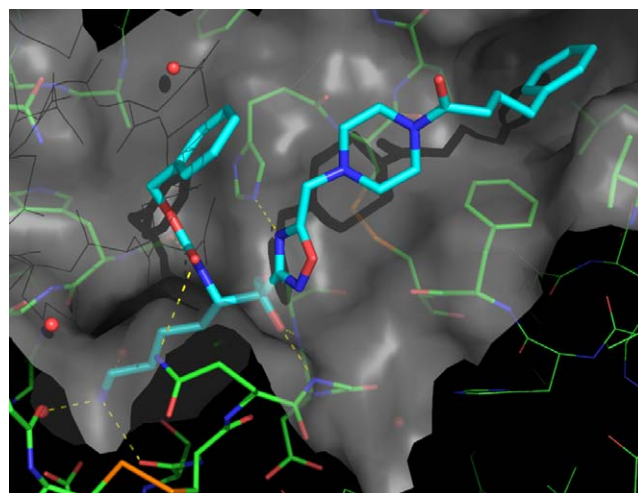
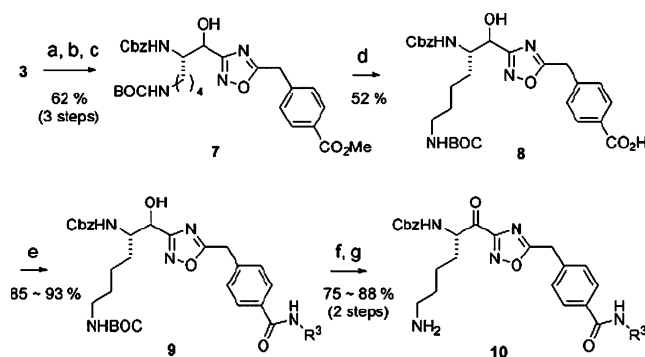


**Figure 2.** X-ray crystal structure of **6c** bound to human  $\beta$ -tryptase.

The synthesis of inhibitors **10** containing a benzamide group is outlined in Scheme 2. Compound **3** was transformed to **7** as shown in Scheme 2. Saponification of the ester **7** was followed by amide coupling reaction with water-soluble carbodiimide reagent (EDCI, HOBT,



**Scheme 2.** Reagents and conditions: (a)  $\text{NH}_2\text{OH}$ , EtOH; (b) 4-( $\text{CO}_2\text{Me}$ )- $\text{PhCH}_2\text{CO}_2\text{H}$  (**4**), HATU, DMF; (c) 100 °C, DMF; (d) LiOH, aq THF; (e)  $\text{R}^3\text{NH}_2$ , EDCI, HOBT, DMF; (f) Dess–Martin periodinane,  $\text{CH}_2\text{Cl}_2$ ; (g) HCl,  $\text{CH}_3\text{CN}$ .

**Table 1.** Structure–activity relationship of tryptase inhibitors **6** containing the piperazine linkage

Compounds	$\text{R}^2$	$\beta$ -Tryptase $K_i$ (nM)	Trypsin $K_i$ (nM)	Solubility ( $\mu\text{M}$ ) at pH 7.4	Microsome stability <sup>a</sup> (%)
<b>6a</b>		470	42	ND	ND
<b>6b</b>		230	33	ND	ND
<b>6c</b>		34	22	>500	2.0
<b>6d</b>		11	11	329	ND
<b>6e</b>		5.8	12	466	22

ND, not detected.

<sup>a</sup> Microsome stability is measured as percent of parent compound remaining after 1 h incubation with human liver microsomes as determined by HPLC.

DMF) to provide the series of compounds **9**. Alcohols **9** were oxidized with Dess–Martin periodinane in dichloromethane,<sup>11</sup> which significantly reduced racemization at the  $\alpha$ -position of the ketone compared to other oxidation conditions. Final deprotection of the BOC group (HCl(g), CH<sub>3</sub>CN) from the lysine side chain provided the series of compounds **10**.

Table 2 shows the structure–activity relationship of inhibitors **10** which have a P1 (L)-Lys and a P2 Cbz group. The initial compound **10a** showed 20-fold improved tryptase potency compared with compound **1a**, but this was not further improved in analogs **10b**, **10c** or **10d**. Increasing the chain length between the amide and the phenyl-capping group such as

**Table 2.** Structure–activity relationship of the benzamide inhibitors **10** in the prime-side distal-pocket binding region

Compounds	R <sup>3</sup> NH <sub>2</sub>	$\beta$ -Tryptase $K_i$ (nM)	Trypsin $K_i$ (nM)	Selectivity	Solubility ( $\mu$ M) at pH 7.4
<b>10a</b>		37	23	0.62	459
<b>10b</b>		39	34	0.87	245
<b>10c</b>		11	15	1.4	100
<b>10d</b>		13	26	2.0	77.2
<b>10e</b>		3.2	20	6.3	440
<b>10f</b>		3.0	19	6.3	370
<b>10g</b>		60	14	0.23	188
<b>10h</b>		140	3.7	0.026	472
<b>10i</b>		3.6	18	5.0	226
<b>10j</b>		220	27	0.12	227
<b>10k</b>		8.2	30	3.7	284
<b>10l</b>		3.5	18	5.1	333
<b>10m</b>		16	31	1.9	ND
<b>10n</b>		1.8	23	13	109
<b>10o</b>		2.9	11	3.8	299
<b>10p</b>		2.4	13	5.4	484
<b>10q</b>		9.9	29	2.9	364
<b>10r</b>		3.7	21	5.7	206

compounds **10e–g**, **10e** and **10f** resulted in 10-fold increase in trypsin potency from **10a**. We then chose **10e** for further optimization to achieve not only better trypsin potency but also selectivity against other antitargets. **10n** with an *m*-chlorophenyl group showed  $K_i$  below 2 nM of trypsin inhibition and 13-fold selectivity over trypsin. Compound **10q** demonstrates that aliphatic end cap groups can also bind in the distal pocket. We were pleased to find that most of compounds **10** in the benzamide series showed high kinetic solubility at pH 7.4 and very low affinity for the hERG  $K^+$  channel.<sup>12</sup>

However, selectivity versus trypsin was still very low. This may not be unexpected since compounds **10** are very flexible and have many different conformers due to the rotational freedom between the activated carbonyl and the oxadiazole ring. In addition, we observed there was poorly defined electron density around the P2 in the crystal structures of **6c** and **10e**, and speculated that the P2 residue might not be making a good interaction with the S2 pocket of trypsin. We decided to synthesize a series of P2 analogs **11** to improve selectivity without reducing trypsin binding affinity. Synthesis of **11a–h** was achieved by using a modification of the sequence in Scheme 2.

The selectivity against trypsin is significantly improved by replacing the Cbz group of **10n** with the shorter ethyl

carbamate (EOC) group of **11a** (Table 3). Substituted benzamides and aliphatic amides also provided improved selectivity against trypsin, ranging from 130- to 270-fold. Among them, difluorobenzamides **11d** and **11e** had over 250-fold selectivity. We speculate that the smaller P2 residues may reduce trypsin affinity due to the weaker hydrophobic interaction at S2 pocket of trypsin. In addition, the less flexible P2 residue may further increase selectivity possibly by steric interactions with Leu99 in trypsin, but not the smaller Ala97 in trypsin.

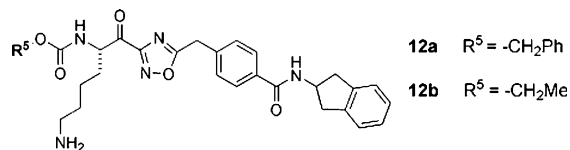
Further optimization led to **12b** in Table 4, which shows very good selectivity over all of the serine proteases. Replacement of the benzyl group **12a** with the ethyl group **12b** improved not only trypsin selectivity more than 10-fold, but also kinetic solubility to over 500  $\mu$ M at pH 7.4. Further evaluation of **12b** also revealed increased microsomal stability compared to **6c**.

While further optimization of P2 is needed, we were able to obtain an X-ray co-crystal structure of **12b** with human  $\beta$ -trypsin (Fig. 3).<sup>13</sup> The activated ketone is covalently linked with the hydroxyl group of Ser195. The nitrogen of the oxadiazole ring forms hydrogen-bonding interaction with His57. The  $\epsilon$ -amino group of lysine residue of **12b** interacts with Asp189 at S1 pocket through a salt-bridge. The benzamide NH- of **12b** is well positioned for hydrogen bonding with the carbonyl group of Cys 58.

Table 3. Structure–selectivity relationship of **11** in the P2 side

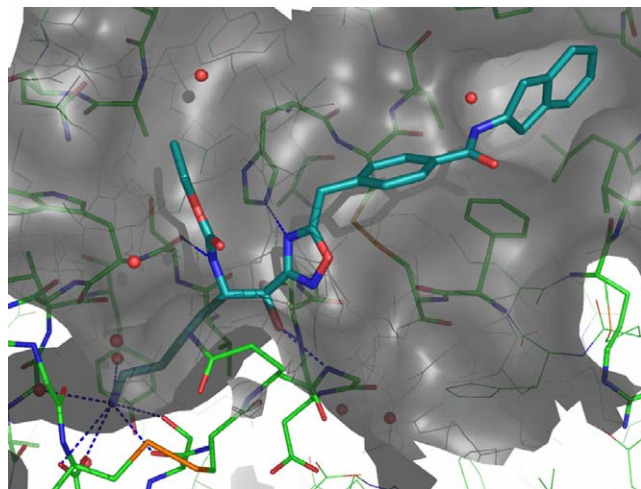
Compounds	R <sup>4</sup>	$\beta$ -Tryptase $K_i$ (nM)	Trypsin $K_i$ (nM)	Selectivity	Solubility ( $\mu$ M) at pH 7.4
<b>11a</b>		1.9	180	95	471
<b>11b</b>		1.8	240	133	390
<b>11c</b>		1.7	280	165	422
<b>11d</b>		1.7	440	265	349
<b>11e</b>		1.5	410	273	313
<b>11f</b>		1.9	330	174	ND
<b>11g</b>		2.1	330	157	337
<b>11h</b>		2.0	470	235	30

ND, not detected.

**Table 4.** Serine proteases selectivity and stability data for **12a** and **12b**

Compounds	$\beta$ -Trypsin $K_i$ (nM)	Trypsin $K_i$ (nM)	Thrombin $K_i$ (nM)	FVIIA $K_i$ (nM)	FXA $K_i$ (nM)	Microsome stability (%)
<b>12a</b>	3.7	21	48,000	140,000	100,000	ND
<b>12b</b>	2.8	170	60,000	>150,000	140,000	64

ND, not detected.

**Figure 3.** X-ray crystal structure of **12b** bound to human  $\beta$ -tryptase.

The phenyl-capping group of **12b** is able to have van der Waals interaction with a unique hydrophobic pocket consisting of a loop (Val59–Leu64) and two  $\beta$ -sheets (Leu33–Gly37 and Tyr37B–Phe41) of  $\beta$ -tryptase. In comparison, trypsin has no specific pocket in this area since hydrogen bonding between the backbones of Phe41 and Lys60 prevents the formation of a well-defined pocket.

In summary, we have achieved highly potent and selective inhibitors of human tryptase with good water solubility. Significant improvements in microsomal stability and hERG channel binding were also demonstrated in analogs from the benzamide series relative to previously described analogs. X-ray co-crystal structures of two amide-containing analogs typifying the series confirmed that the molecules are capable of occupying a distal binding pocket in tryptase that is thought to be important for potency and selectivity.

#### Acknowledgment

The authors thank Joseph D. Ho for his contribution to X-ray crystallography work, which was conducted

at the Advanced Light Source (ALS) in the Lawrence Berkeley Laboratory.

#### References and notes

- Clark, J. M.; Abraham, W. M.; Fishman, C. E.; Forteza, R.; Ahmed, A.; Cortes, A.; Warne, R. L.; Moore, W. R.; Tanaka, R. D. *Am. J. Respir. Crit. Care Med.* **1995**, *152*, 2076.
- Pereira, P. J. B.; Bergner, A.; Macedo-Ribeiro, S.; Huber, R.; Matschiner, G.; Fritz, H.; Sommerhoff, C. P.; Bode, W. *Nature* **1998**, *392*, 306.
- Sommerhoff, C. P. *Am. J. Respir. Crit. Care Med.* **2001**, *164*, S52.
- Costanzo, M. J.; Yabut, S. C.; Almond, H. R., Jr.; Andrade-Gordon, P.; Corcoran, T. W.; de Garavilla, L.; Kauffman, J. A.; Abraham, W. M.; Recacha, R.; Chattopadhyay, D.; Maryanoff, B. E. *J. Med. Chem.* **2003**, *46*, 3865.
- (a) Hopkins, C. R.; Czekaj, M.; Kaye, S. S.; Gao, Z.; Pribish, J.; Pauls, H.; Liang, G.; Sides, K.; Cramer, D.; Cairns, J.; Luo, Y.; Lim, H.-K.; Vaz, R.; Robello, S.; Maignan, S.; Dupuy, A.; Mathieu, M.; Levell, J. *Bioorg. Med. Chem. Lett.* **2005**, *15*, 2734; (b) Zhao, G.; Bolton, S. A.; Kwon, C.; Hartl, K. S.; Seiler, S. M.; Slusarchyk, W. A.; Sutton, J. C.; Bisacchi, G. S. *Bioorg. Med. Chem. Lett.* **2004**, *14*, 309.
- De Ponti, F.; Poluzzi, E.; Cavalli, A.; Recanatini, M.; Montanaro, N. *Drug Saf.* **2002**, *25*, 263.
- (a) Lipinski, C. A.; Lombardo, F.; Dominy, B. W.; Feeney, P. J. *Adv. Drug Delivery Rev.* **1997**, *23*, 3; (b) van de Waterbeemd, H.; Smith, D. A.; Beaumont, K.; Walker, D. K. *J. Med. Chem.* **2001**, *44*, 1313.
- Tavares, F. X.; Deaton, D. N.; Miller, A. B.; Miller, L. R.; Wright, L. L. *Bioorg. Med. Chem. Lett.* **2005**, *15*, 3891.
- Evans, M. D.; Ring, J.; Schoen, A.; Bell, A.; Edwards, P.; Berthelot, D.; Nicewonger, R.; Baldino, C. M. *Tetrahedron Lett.* **2003**, *44*, 9337.
- Mancuso, A. J.; Brownfain, D. S.; Swern, D. *J. Org. Chem.* **1979**, *44*, 4148.
- Dess, D. B.; Martin, J. J. *J. Org. Chem.* **1983**, *48*, 4155.
- Compounds **10p** and **10q** show 7.2% at 10  $\mu$ M and 0% hERG channel binding at 1  $\mu$ M substrate concentration, respectively.
- The tryptase crystal structures have been deposited in the Protein Data Bank (PDB) under Accession codes 2GDD and 2FS9.